BAG3 directly stabilizes Hexokinase 2 mRNA and promotes aerobic glycolysis in pancreatic cancer cells

Ming-Xin An,[1,2,3] Si Li,[1] Han-Bing Yao,[1] Chao Li,[1] Jia-Mei Wang,[1] Jia Sun,[1] Xin-Yu Li,[1] Xiao-Na Meng,[1] and Hua-Qin Wang[1,2,3]

[1]Department of Biochemistry and Molecular Biology, [2]Key Laboratory of Cell Biology, Ministry of Public Health, and [3]Key Laboratory of Medical Cell Biology, Ministry of Education, China Medical University, Shenyang, China

Aerobic glycolysis, a phenomenon known historically as the Warburg effect, is one of the hallmarks of cancer cells. In this study, we characterized the role of BAG3 in aerobic glycolysis of pancreatic ductal adenocarcinoma (PDAC) and its molecular mechanisms. Our data show that aberrant expression of BAG3 significantly contributes to the reprogramming of glucose metabolism in PDAC cells. Mechanistically, BAG3 increased Hexokinase 2 (HK2) expression, the first key enzyme involved in glycolysis, at the posttranscriptional level. BAG3 interacted with HK2 mRNA, and the degree of BAG3 expression altered recruitment of the RNA-binding proteins Roquin and IMP3 to the HK2 mRNA. BAG3 knockdown destabilized HK2 mRNA via promotion of Roquin recruitment, whereas BAG3 overexpression stabilized HK2 mRNA via promotion of IMP3 recruitment. Collectively, our results show that BAG3 promotes reprogramming of glucose metabolism via interaction with HK2 mRNA in PDAC cells, suggesting that BAG3 may be a potential target in the aerobic glycolysis pathway for developing novel anticancer agents.

Introduction

It has been widely recognized that reprogramming cellular metabolism is one of characteristic hallmarks of cancer cells and contributes to tumor development (Cairns et al., 2011; Hanahan and Weinberg, 2011). In contrast with normal cells, most cancer cells primarily rely on aerobic glycolysis for glucose metabolism even under normoxic conditions, a metabolic phenomenon known as the Warburg effect (Vander Heiden et al., 2009). Aerobic glycolysis allows cancer cells to coordinate their energetic demands and precursor materials used in macromolecule synthesis, thereby fueling the rapid growth and proliferation observed in tumors (DeBerardinis and Thompson, 2012). Aberrant regulation of glycolytic enzymes is partly responsible for metabolic shift to aerobic glycolysis to facilitate cancer progression (Gatenby and Gillies, 2004). Hexokinases (HKs) are involved in almost all glucose metabolism by catalyzing the essentially irreversible first step of glucose metabolism in cells. Four HK isoforms (HK1–HK4) encoded by discrete genes have been identified in mammalian tissues. Most normal mammalian tissues express very little HK2, whereas its expression is highly up-regulated in various types of tumors, including pancreatic tumors (Anderson et al., 2016; Liu et al., 2016; Penny et al., 2016).

BAG3 is a member of the human Bcl-2–associated athanogene (BAG) cochaperone family (BAG1–6), which interacts with the ATPase domain of the heat shock protein 70 (HSP70) through the evolutionarily conserved BAG domain (Takayama et al., 1999). In addition to the BAG domain, BAG3 contains a WW domain and a proline-rich repeat (PxxP), both of which appear to permit it to interact with discrete proteins (Rosati et al., 2011). Because of the adapter nature of its multidomain structure, BAG3 is assigned to play a wide portfolio of the regulatory function such as apoptosis, development, cytoskeleton arrangement, and autophagy (Rosati et al., 2011; Behl, 2016). Recent literature describes that BAG3 is often overexpressed in many cancers, and its expression is correlated with the poor prognosis of some cancers, such as pancreatic, glioblastoma, and thyroid (Liao et al., 2001; Romano et al., 2003a,b; Chiappetta et al., 2007; Rosati et al., 2007; Festa et al., 2011; Suzuki et al., 2011; Felzen et al., 2015; Sherman and Gabai, 2015). However, the oncogenic potential of BAG3 remains incompletely understood.

Both transcriptional and posttranscriptional mechanisms are implicated in altering gene expression in cells. Recruitment of protein is implicated in every aspect of RNA life, from biosynthesis to degradation. In eukaryotic cells, the interaction of RNA-binding proteins (RBPs) with their cognate RNAs leads to the formation of ribonucleoprotein particles (RNPs), thereby regulating multiple posttranscriptional pro-

Correspondence to Hua-Qin Wang: hqwang@cmu.edu.cn

Abbreviations used: 3-BrPA, 3-bromopyruvic acid; BAG, Bcl-2–associated athanogene; CDE, constitute degradation element; CR, coding region; ECAR, extracellular acidification rate; gRNA, guide RNA; HK, Hexokinase; KI, knock-in; MEF, mouse embryonic fibroblast; OCR, oxygen consumption rate; PDAC, pancreatic ductal adenocarcinoma; PLA, proximity ligation assay; RBP, RNA-binding protein; RIP, RNA immunoprecipitation; RNP, ribonucleoprotein particle; RT-qPCR, reverse transcription quantitative PCR; RTCA, real-time cell analysis.

The Rockefeller University Press
J. Cell Biol. Vol. 216 No. 12 4091–4105
https://doi.org/10.1083/jcb.201701064

cesses (Müller-McNicoll and Neugebauer, 2013). Throughout their life in the nucleus and the cytoplasm, mRNAs are constantly associated with a variable set of proteins that influence the fate of the mRNA (Müller-McNicoll and Neugebauer, 2013). Therefore, the interplay between RNAs and RNPs determines the fate of an mRNA.

In this study, we show a new mechanism of BAG3 that facilitates proliferation of pancreatic ductal adenocarcinomas (PDACs) and promotes reprograming of glucose metabolism by stabilization of HK2 mRNA via competition with Roquin and cooperation with IMP3 to interact with the HK2 transcript. Thereby, we give new insights into the complex posttranscriptional regulation of HK2 by BAG3 in PDACs. Notably, we also discovered the first cellular mechanism involving BAG3 functions as an RBP, indicating that BAG3 might serve as a potential pharmaceutical target for cancer treatment.

Results

BAG3 affects the proliferative rate of PDACs

BAG3 expression was evaluated by immunohistochemical analysis in pancreatic cancer specimens, and we confirmed that BAG3 expression was significantly increased in most tumor specimens relative to peritumor tissues (Fig. 1, A and B). BAG3 immunostaining signals were primarily detected in cytoplasm (Fig. 1 A). Importantly, patients with high BAG3 intensity showed significantly worse overall survival (Fig. 1 C). The Cox proportional hazards model revealed that high BAG3 was an independent prognostic factor with respect to overall survival (hazard ratio = 3.512 [95% confidence interval; 2.667–6.981]; $P < 0.0001$). To investigate the potential involvement of BAG3 in PDACs, BAG3 was knocked down using the CRISPR/Cas9 system, and two constructs, PCA00136 and PCA00137, significantly decreased BAG3 expression in BxPC3 cells (Fig. 1 D). Real-time cell analysis (RTCA; Fig. 1 E), Edu incorporation (Fig. 1 F), and cell number count (Fig. 1 G) demonstrated that knockdown of BAG3 inhibited proliferation of BxPC3 cells. BAG3 was also knocked down in SW1990 cells (Fig. 1 H), and RTCA demonstrated that BAG3 knockdown also prohibited proliferation of SW1990 cells (Fig. 1 I). BAG3 knockdown did not increase apoptosis of either BxPC3 or SW1990 cells, as assessed by Annexin V and propidium iodide staining, followed by flow cytometry (not depicted). To exclude the potential off-target effects, expression of some BAG family members was analyzed, and we demonstrated that BAG3 knockdown had no effect on expression of BAG2 or BAG6 (Fig. 1, D and H). Consistent with the previously reported negative correlation of BAG1 and BAG3 expression in other cell types (Gamerdinger et al., 2009; Meng et al., 2014), BAG3 knockdown increased BAG1 expression in PDAC cells (Fig. 1, D and H). Xenograft experiments were further performed and demonstrated that knockdown of BAG3 suppressed primary tumor growth in humanized mice (Fig. 1 J).

BAG3 knockdown suppresses glycolysis of PDACs

To get a first insight into a potential involvement of BAG3 in metabolic regulation of PDACs, the oxygen consumption rate (OCR), as an indicator of cellular respiration, was analyzed in PDACs after serial addition of oligomycin, p-trifluoromethoxy carbonylcyanide phenylhydrazone (FCCP), and antimycin A. PCA00136 guide RNA (gRNA)-guided BAG3 knockdown resulted in higher OCR in BxPC3 (Fig. 2 A) and SW1990 (Fig. 2 B) cells. Similar results were obtained using another gRNA, PCA00137 (Fig. S1, A and B). The extracellular acidification rate (ECAR) was also analyzed after serial addition of glucose, oligomycin, and 2-deoxyglucose. On the contrary, ECAR was significantly decreased in BxPC3 (Fig. 2 C) and SW1990 (Fig. 2 D) cells infected with PCA00136. PCA00137 gRNA-guided BAG3 knockdown also decreased ECAR in BxPC3 (Fig. S1 C) or SW1990 (Fig. S1 D) cells. Extracellular glucose analysis demonstrated that BAG3 knockdown suppressed glucose consumption by BxPC3 (Fig. 2 E) and SW1990 (Fig. 2 F) cells. Extracellular lactate level as a surrogate indicator of glycolysis was also measured, and a significant decrease of extracellular lactate secretion was observed in BxPC3 (Fig. 2 G) and SW1990 (Fig. 2 H) cells with BAG3 knockdown.

Ectopic BAG3 overexpression promotes glycolysis of PDACs

To further confirm the potential involvement of BAG3 in glycolysis, BAG3 was overexpressed in PDACs (Fig. 3 A). Contrary to BAG3 knockdown, forced overexpression of BAG3 decreased OCR in BxPC3 (Fig. 3 B) and SW1990 (Fig. 3 C) cells, whereas it increased ECAR in BxPC3 (Fig. 3 D) and SW1990 (Fig. 3 E) cells. Glucose consumption was accelerated by forced BAG3 expression in BxPC3 (Fig. 3 F) and SW1990 (Fig. 3 G) cells. In addition, forced BAG3 expression also increased extracellular lactate secretion in BxPC3 (Fig. 3 H) and SW1990 (Fig. 3 I) cells. RTCA demonstrated that up-regulation of BAG3 promoted proliferation of BxPC3 (Fig. 3 J) and SW1990 (Fig. 3 K) cells.

BAG3 regulates HK2 mRNA stability via its 3′UTR independent of miRNAs in PDACs

The findings that increase in glycolysis by BAG3 prompted us to ask whether BAG3 regulates the expression of genes related to glucose metabolism, and we found that BAG3 knockdown significantly decreased HK2 expression in both BxPC3 and SW1990 cells (Fig. 4 A). Reverse transcription quantitative PCR (RT-qPCR) demonstrated that BAG3 knockdown decreased HK2 mRNA in BxPC3 and SW1990 cells (Fig. 4 B). However, novel HK2 mRNA synthesis using a Click-iT nascent RNA capture system demonstrated that no obvious alteration was observed in BxPC3 and SW1990 cells with BAG3 knockdown (Fig. 4 C). Actinomycin D was also used to block de novo RNA synthesis, and the persistence of the existing HK2 mRNA was measured by RT-qPCR. BAG3 knockdown promoted degradation of the HK2 mRNA in BxPC3 (Fig. 4 D) and SW1990 (Fig. 4 E) cells. On the contrary, RT-PCR demonstrated that forced BAG3 expression increased HK2 mRNA in BxPC3 and SW1990 (Fig. 4 F). Consistent with mRNA expression, forced BAG3 expression increased HK2 protein levels in PDAC cells (Fig. 4 G). HK2 activity was then inhibited using 3-bromopyruvic acid (3-BrPA). RTCA demonstrated that 3-BrPA suppressed cell index in both BxPC3 (Fig. 4, H and J) and SW1990 (Fig. 4, I and K) cells. The suppressive effect of 3-BrPA was compromised in BAG3-knockdown cells (Fig. 4, H and I), whereas it was enhanced in forced BAG3 expression cells (Fig. 4, J and K). OCR was suppressed by 3-BrPA in BxPC3 (Fig. S2 A) and SW1990 (Fig. S2 B) cells. In the presence of 3-BrPA, PDAC

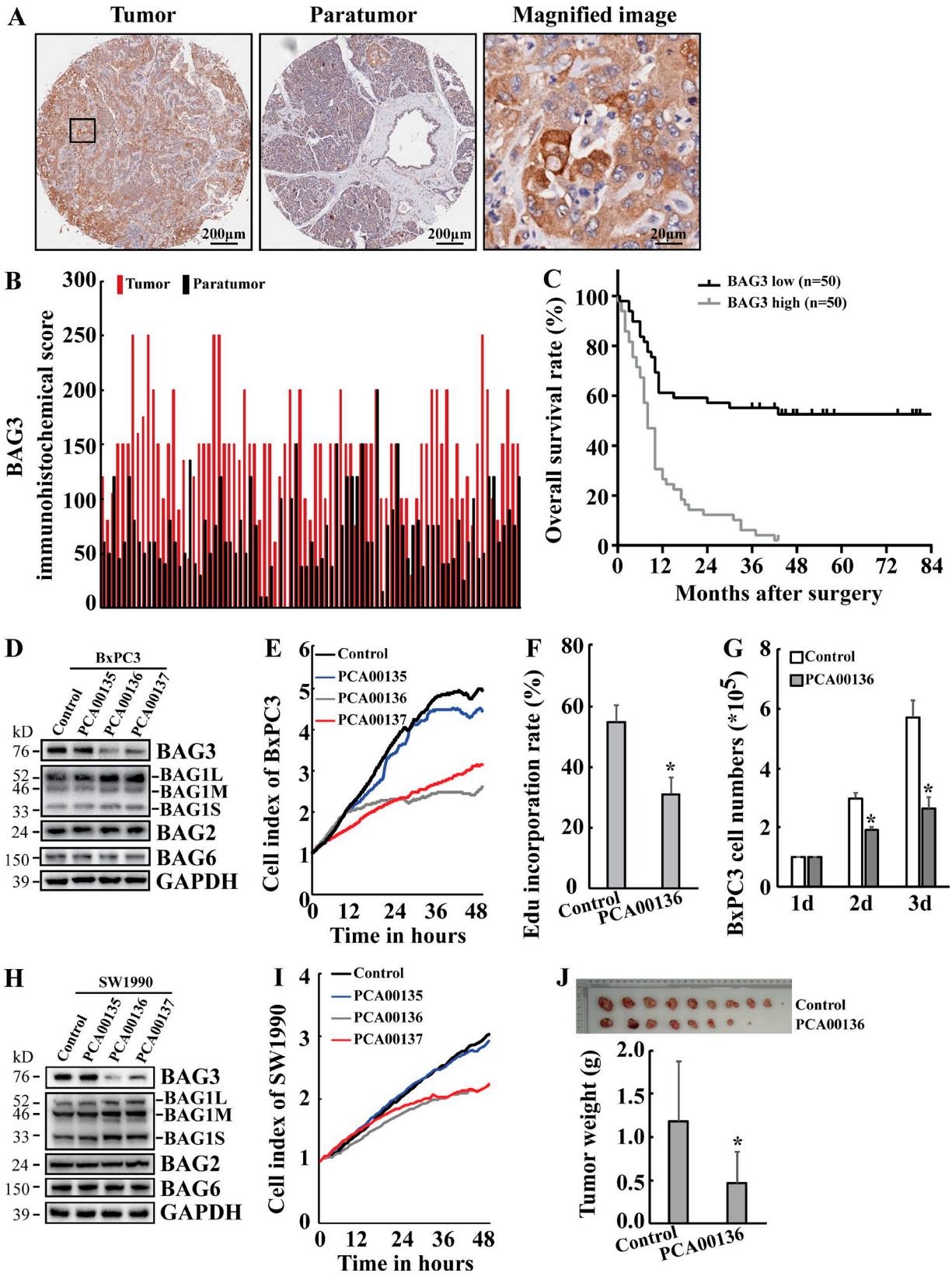

Figure 1. **BAG3 knockdown suppresses proliferation of PDACs.** (A and B) Pancreatic cancer tissue chip was immunohistochemically stained using BAG3 antibody. Representative immunohistochemical images were provided (A), and immunohistochemical intensity was scored (B). (C) Kalpan-Meier plot indicating the overall survival of patients with pancreatic cancer categorized by BAG3 expression. P-values were determined by log-rank test. (D) BxPC3 cells were infected with gRNA-guided BAG3 using the CRISPR/Cas9 system. Western blotting was performed using the indicated antibodies. (E) Control or BAG3-knockdown BxPC3 cells were plated on an E plate, and real-time cell indexes were analyzed using RTCA. (F) De novo DNA synthesis was analyzed using Edu incorporation in control or BAG3-knockdown BxPC3 cells. (G) Control or BAG3-knockdown BxPC3 cells were plated on six-well plates, and cell

cells with BAG3 knockdown demonstrated similar OCR with their control partner (Fig. S2, A and B). 3-BrPA also suppressed ECAR in BxPC3 (Fig. S2 C) and SW1990 (Fig. S2 D) cells. In addition, PDAC cells with BAG3 knockdown demonstrated comparable ECAR with their control partner in the presence of 3-BrPA (Fig. S2, C and D).

To examine which region is ascribed to regulation of HK2 mRNA by BAG3, the 5′UTR, coding region (CR), and 3′ UTR of an HK2 gene fragment was fused after the stop codon of luciferase gene, and then the luciferase activity was measured. When compared with control cells, BxPC3 cells with BAG3 knockdown demonstrated significant reduction in the luciferase activity of the construct containing 3′UTR of HK2 gene (Fig. 4 L). Insertion of 5′UTR or CR of the HK2 gene demonstrated no difference of luciferase activity in control and BAG3-knockdown cells (Fig. 4 L). On the contrary, luciferase activity of the construct containing 3′UTR was significantly increased in BxPC3 cells with forced BAG3 expression (Fig. 4 M). These data indicate that BAG3 regulates HK2 mRNA stability via its 3′UTR. miRNAs control the target RNA stability and translation by their recruitment to the 3′UTR (Fabian et al., 2010). To explore the possible involvement of miRNAs, HK2 mRNA was immunoprecipitated with antibody against Argonaute 2 (Ago2), the essential effector of miRNA-induced gene silencing. No obvious interaction of Ago2 with HK2 mRNA was observed in either BxPC3 (Fig. S3 A) or SW1990 (Fig. S3 B) cells. In addition, BAG3 knockdown did not alter the recruitment of Ago2 to HK2 mRNA (Fig. S3, A and B). Ago2 was further knocked down using lentivirus containing shRNAs specific against Ago2 (shAgo2). shAgo2 significantly decreased Ago2 mRNA in both control and BAG3-knockdown BxPC3 cells (Fig. S3 C). However, Ago2 knockdown demonstrated no obvious effect on HK2 mRNA levels in either control or BAG3-knockdown cells (Fig. S3 D). Consistent with mRNA expression, Western blotting demonstrated that BAG3 knockdown decreased HK2 expression, which was unaltered by knockdown of Ago2 (Fig. S3 E).

BAG3 directly interacts with 3′UTR of HK2 mRNA via its 67–76 aa and 473–485 aa

Previously, we have globally screened BAG3-interacting proteins by proteomic analysis and investigated the binding proteins of BAG3 (Kong et al., 2013, 2016). Among these candidates, HSP70, nucleolin (NCL), GAPDH, AUF1, IMP1, and IMP3 were assigned to RBPs. RNA immunoprecipitation (RIP) demonstrated more than twofold enrichment of HK2 transcript by IMP1 and HSP70 in BxPC3 cells (Fig. 5 A). We then explored whether BAG3 might stabilize HK2 mRNA via interaction with its transcript. RIP demonstrated more than twofold enrichment of HK2 mRNA by BAG3 in both BxPC3 and SW1990 cells (Fig. 5 B). To explore whether IMP1 or HSP70 might be responsible for BAG3 recruitment to the HK2 transcript, IMP1 or HSP70 was knocked down by lentivirus containing shRNAs specific against IMP1 (shIMP1) or HSP70 (shHSP70). Western blotting demonstrated that shIMP1 or shHSP70 specifically decreased the protein expression of their targets (Fig. 5 C). RIP was then performed in BxPC3 cells and demonstrated that neither IMP1 nor HSP70 knockdown altered recruitment of BAG3 to HK2 transcript (Fig. 5 D). Biotin pull-down was then performed using the in vitro transcribed 5′UTR, CR, or 3′UTR segment of HK2 mRNA. Consistent with luciferase analysis (Fig. 4, L and M), BAG3 was pulled down by the 3′UTR of HK2 mRNA, whereas the 5′UTR or CR segment was unable to pull down BAG3 (Fig. 5 E). HSP70 was also precipitated by 3′UTR of HK2 mRNA, whereas IMP1 was precipitated by both the CR and 3′UTR of HK2 mRNA (Fig. 5 E). Consistent with RIP (Fig. 5 A), GAPDH was not precipitated by any segment of HK2 mRNA (Fig. 5 E). In silico prediction using the Pprint online prediction platform (Kumar et al., 2008) indicated that BAG3 protein contains three potential RNA-binding domains located at 67–76 aa, 261–294 aa, and 473–485 aa. Constructs containing BAG3 with the indicated deletion were then generated, and RIP demonstrated that BAG3-mediated recruitment of HK2 transcript was significantly reduced by mutation with 67–76 aa or 473–485 aa deletions (Fig. 5 F). RT-qPCR demonstrated that BAG3 increased HK2 mRNA levels, which was partly suppressed by deletion of 67–76 aa or 473–485 aa (Fig. 5 G). In contrast, BAG3-mediated up-regulation of the HK2 transcript was unaltered by deletion of 261–294 aa (Fig. 5 G). Consistent with mRNA expression, Western blotting demonstrated that BAG3 increased HK2 protein expression, which was unaltered by deletion of its 261–294 aa (Fig. 5 H). However, deletion of 67–76 aa or 473–485 aa partly blocked the promotive effect of BAG3 (Fig. 5 H). As 473–485 aa is located in the BAG domain, immunoprecipitation was also performed. Interaction of BAG3 with HSP70 was blocked by BAG3 with 473–485 aa deletion, whereas interaction of BAG3 with IMP1 was unaltered (Fig. 5 I). Deletion of 67–76 aa or 261–294 aa did not alter the interaction between BAG3 with HSP70 or IMP1 (Fig. 5 I). RIP demonstrated that recruitment of neither IMP1 (Fig. 5 J) nor HSP70 (Fig. 5 K) was altered by intact or mutant BAG3.

BAG3 interacts with constitute degradation element (CDE), located on the 3′UTR of HK2 mRNA, and prohibits Roquin recruitment

To explore whether BAG3 recruitment might alter other RBP recruitment, RIP was performed using control and BAG3-knockdown BxPC3 cells, and it demonstrated that BAG3 knockdown did not alter the recruitment of RBPs, including IMP1 and HSP70 (Fig. 6 A). Knockdown of IMP1 or HSP70 unaltered HK2 mRNA expression in both control and BAG3-knockdown cells (Fig. 6 B). Western blotting demonstrated that HK2 protein was unaltered by IMP1 knockdown, whereas it was markedly decreased by HSP70 knockdown in both control and BAG3-knockdown cells (Fig. 6 C). Investigation on the 3′UTR of the HK2 gene found a core CDE consensus sequence (UCYRYGA; Leppek et al., 2013) that was present on 2,077–2,083 residues. As Roquin has been previously shown to bind with numerous mRNAs containing CDE to control the degradation of target mRNAs independent of miRNAs (Leppek et al., 2013), we explored whether recruitment of BAG3

numbers were counted daily for 3 d. (H) SW1990 cells were infected with gRNA-guided BAG3 using CRISPR/Cas9 system, and BAG3 expression was confirmed using Western blot. (I) Control or BAG3-knockdown SW1990 cells were plated on an E plate, and real-time cell indexes were analyzed using RTCA. (J) Control or BAG3-knockdown BxPC3 cells were injected intracutaneously into nude mice. Tumors were excised after mice sacrifice on day 28 (n = 10 mice/group). Tumors were photographed (top), and weights were measured (bottom). *, $P < 0.01$. Error bars indicate means ± SD.

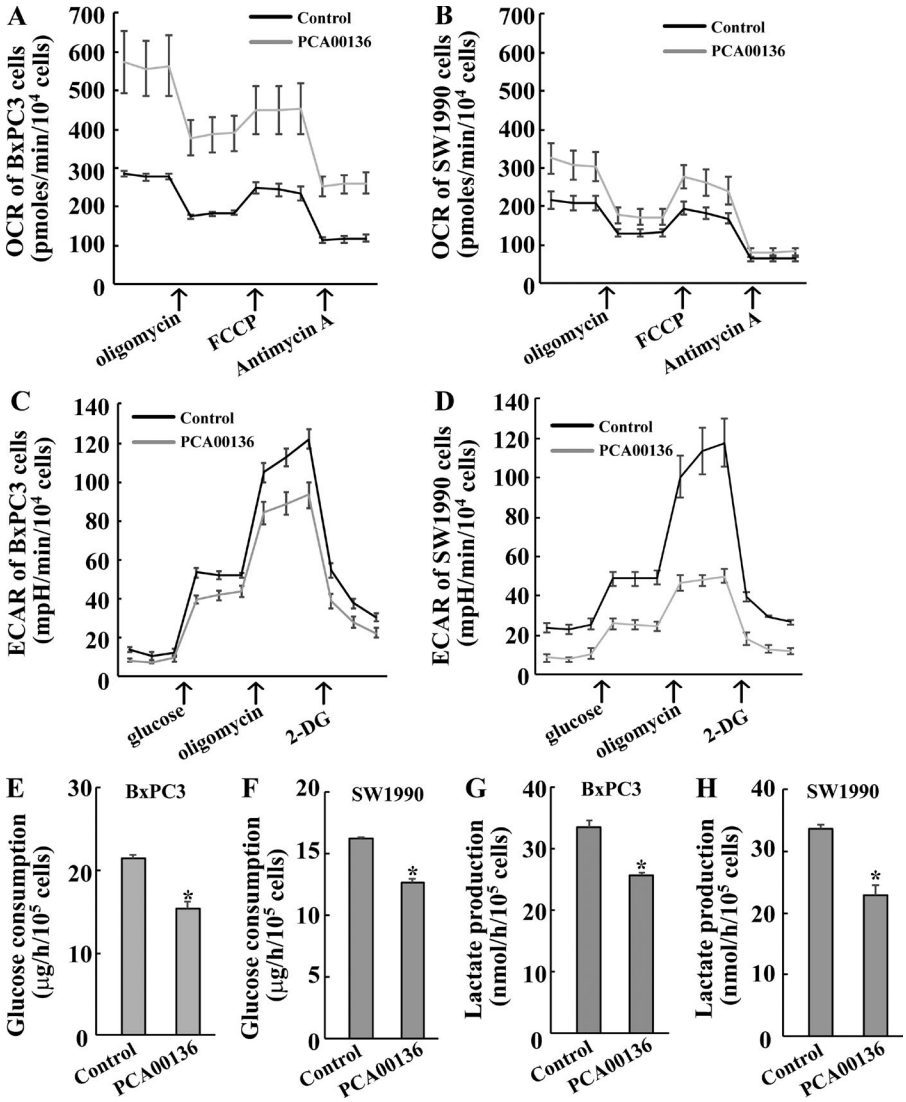

Figure 2. **Knockdown of BAG3 suppresses glycolysis in PDACs.** (A and B) OCR was analyzed using seahorse instrument in control or BAG3-knockdown BxPC3 (A) or SW1990 (B) cells. (C and D) ECAR was analyzed using seahorse instrument in control or BAG3-knockdown BxPC3 (C) or SW1990 (D) cells. 2-DG, 2-deoxyglucose. (E and F) Glucose consumption was analyzed using the colorimetric method in control or BAG3-knockdown BxPC3 (E) or SW1990 (F) cells. (G and H) Extracellular lactate production was analyzed using colorimetric method in control or BAG3-knockdown BxPC3 (G) or SW1990 (H) cells. *, $P < 0.01$. Error bars indicate means ± SD.

might regulate Roquin recruitment. RIP using Roquin antibody demonstrated that Roquin was recruited to HK2 mRNA in BxPC3 or SW1990 cells with BAG3 knockdown, whereas it was not recruited in control BxPC3 or SW1990 cells (Fig. 6 D). To explore whether promotion of Roquin recruitment might ascribe to HK2 down-regulation mediated by BAG3 knockdown, the luciferase construct containing HK2 3′UTR with core CDE mutation was then generated (Fig. 6 E). Luciferase activity assays demonstrated that BAG3 knockdown reduced the luciferase activity of construct with insertion of a WT 3′UTR, whereas it did not alter the luciferase activity of the construct with the insertion of a 3′UTR containing a CDE mutation (Fig. 6 F). To further confirm the involvement of Roquin, Roquin was knocked down using lentivirus containing shRNA specific against Roquin (shRoquin; Fig. 6 G). Roquin down-regulation increased HK2 mRNA in cells with BAG3 knockdown, whereas it demonstrated no alteration of HK2 mRNA expression in control cells (Fig. 6 H). Western blotting confirmed that knockdown of Roquin increased HK2 protein in BxPC3 cells with BAG3 knockdown (Fig. 6 I). Biotin pulldown using WT or mutant 3′UTR was then performed and demonstrated that BAG3 was precipitated by biotin-labeled WT 3′UTR but not mutant 3′UTR (Fig. 6 J). However, the interaction of HK2 mRNA with IMP1 or HSP70 mutation was unaltered by mutation on CDE (Fig. 6 J).

BAG3 interacts with IMP3 and facilitates its recruitment to the 3′UTR of HK2 mRNA

To further confirm whether BAG3 regulates stability of HK2 transcript via interaction, luciferase activity assays were performed in BxPC3 cells with ectopic BAG3 expression, and they demonstrated that BAG3 overexpression increased the luciferase activity of construct containing WT, but not CDE mutant 3′UTR of the HK2 gene (Fig. 7 A). No obvious recruitment of Roquin to the HK2 mRNA was observed in control PDACs (Fig. 6 D), indicating that forced BAG3 overexpression might cooperate with other RBPs to stabilize HK2 mRNA. Therefore, RIP was performed using BxPC3 cells with forced BAG3 overexpression, and it demonstrated that ectopic BAG3 expression markedly increased IMP3 recruitment (Fig. 7 B). IMP3 recruitment was also analyzed using SW1990 cells with forced BAG3 expression, and similar results were obtained (Fig. 7 C). IMP3 and BAG3 was then cotransfected to HEK293 cells, and coimmunoprecipitation demonstrated that BAG3 had interacted with IMP3 (Fig. 7 D). Coimmunoprecipitation also confirmed

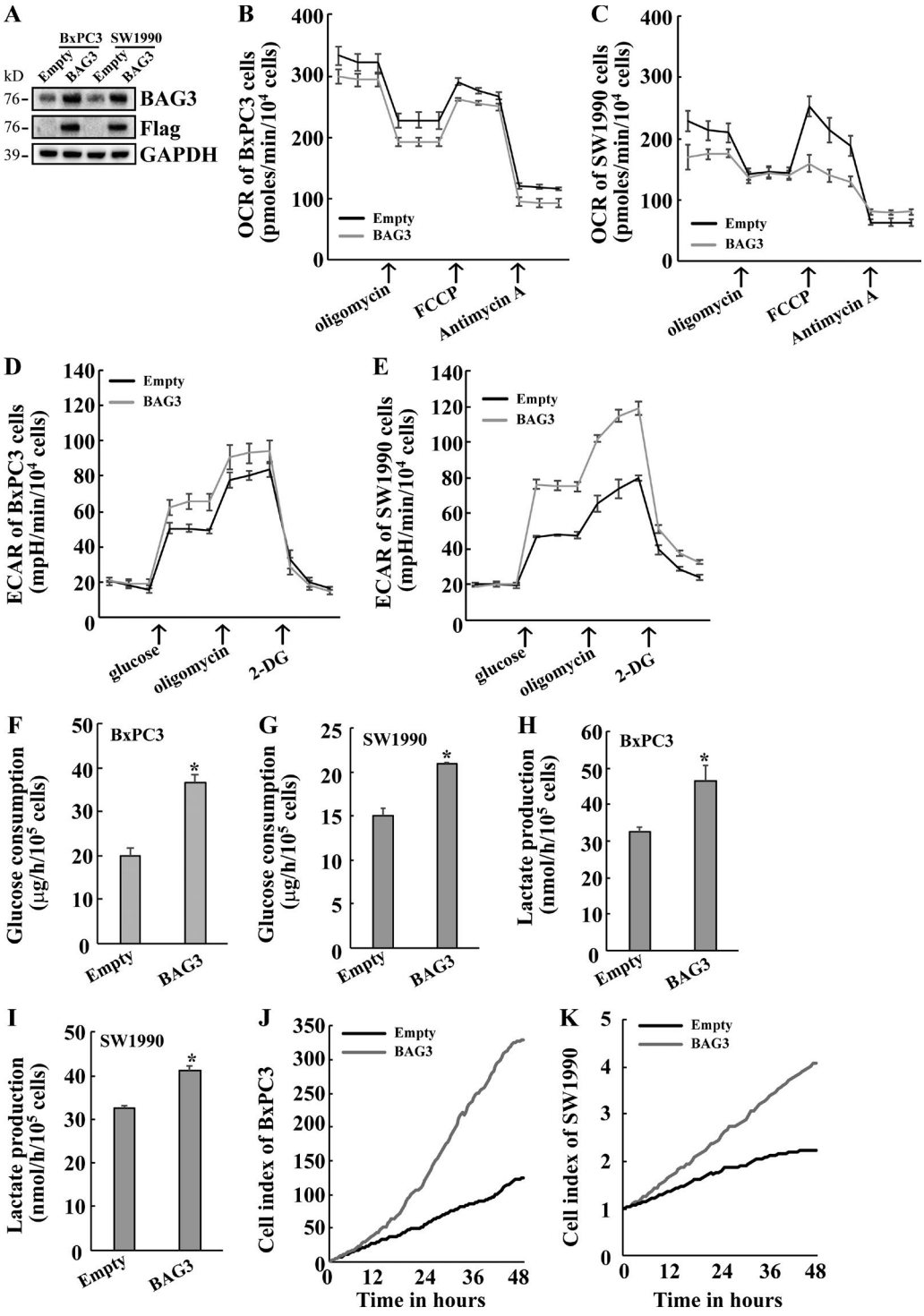

Figure 3. **BAG3 overexpression promotes glycolysis of PDACs.** (A) BxPC3 or SW1990 cells were infected with lentivirus containing empty or BAG3 construct. BAG3 expression was confirmed using Western blotting. (B and C) BxPC3 (B) or SW1990 (C) cells were infected with lentivirus containing empty or BAG3 construct, and OCR was analyzed using seahorse instrument. (D and E) BxPC3 (D) or SW1990 (E) cells were infected with lentivirus containing empty or BAG3 construct, and ECAR was analyzed using seahorse instrument. 2-DG, 2-deoxyglucose. (F and G) BxPC3 (F) or SW1990 (G) cells were infected with lentivirus containing empty or BAG3 construct, and glucose consumption was analyzed using colorimetric method. (H and I) BxPC3 (H) or SW1990 (I) cells were infected with lentivirus containing empty or BAG3 construct, and extracellular lactate production was analyzed using the colorimetric method. (J and K) BxPC3 (J) or SW1990 (K) cells infected with lentivirus containing empty or BAG3 construct were plated on E plate, and real-time cell indexes were analyzed using RTCA. *, $P < 0.01$. Error bars indicate means ± SD.

interaction of endogenous BAG3 and IMP3 in BxPC3 and SW1990 cells (Fig. 7 E). GST pulldown demonstrated no interaction of BAG3 with IMP3 using recombinant proteins (not depicted). However, DuoLink proximity ligation assay (PLA) demonstrated direct interaction of endogenous BAG3 and IMP3 in BxPC3 and SW1990 cells (Fig. 7 F). To investigate

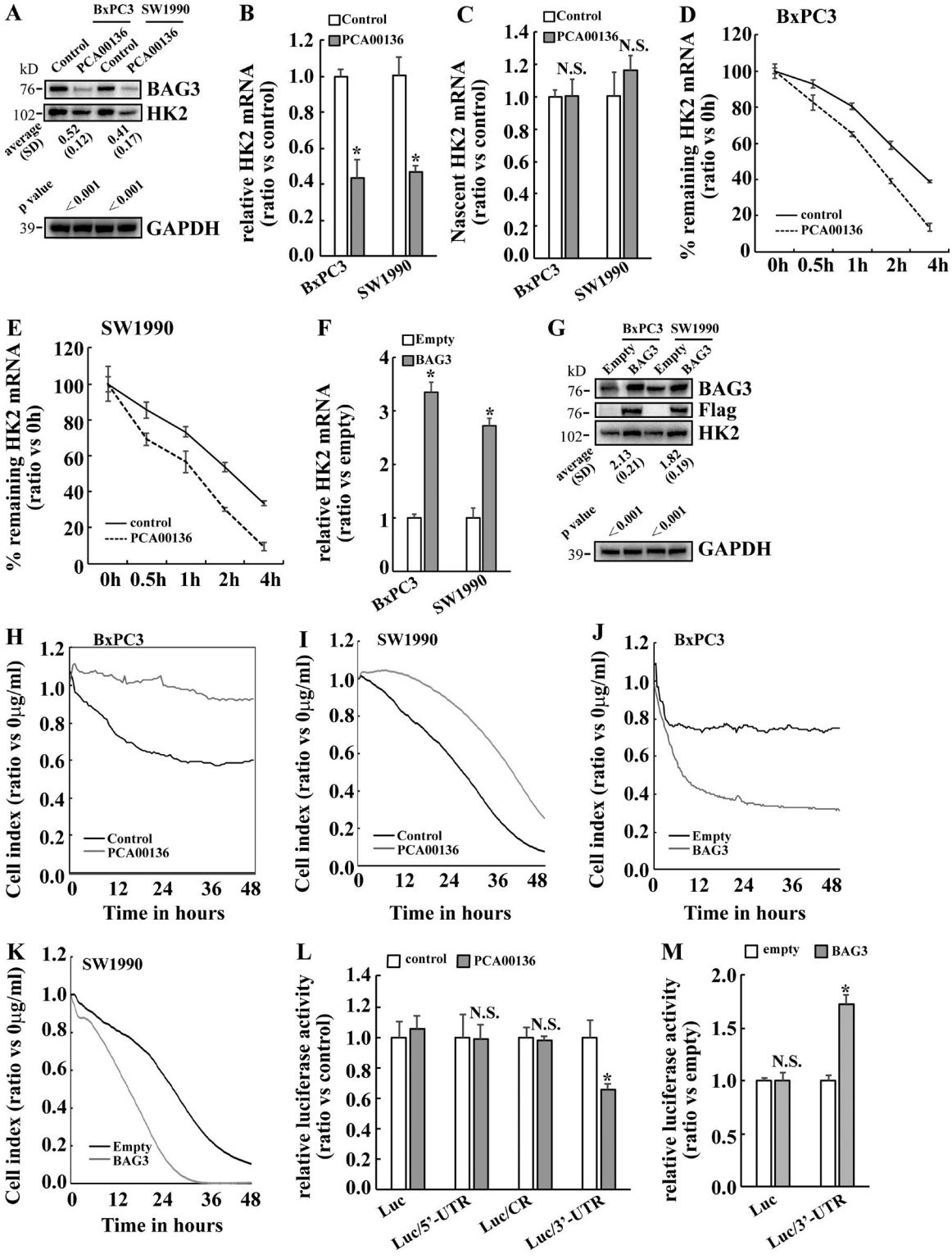

Figure 4. **BAG3 regulates turnover of HK2 mRNA via its 3′UTR.** (A) HK2 expression was analyzed using lysates from control or BAG3-knockdown BxPC3 or SW1990 cells. A representative image was presented, and the ratio of HK2 expression (normalized by GAPDH; ratio in control cells was defined as 1.0) was noted at the bottom of the image (n = 3). (B) HK2 mRNA was analyzed using RT-PCR in control, BAG3-knockdown BxPC3, or SW1990 cells. (C) Nascent RNA was labeled and isolated, and newly synthesized HK2 mRNA was analyzed using RT-PCR in control or BAG3-knockdown BxPC3 or SW1990 cells. (D and E) Actinomycin D was added for the indicated period to block RNA synthesis, and HK2 mRNA was analyzed using RT-PCR in control or BAG3-knockdown BxPC3 (D) or SW1990 (E) cells. (F) BxPC3 or SW1990 cells were infected with lentivirus containing empty or BAG3 construct. HK2 mRNA was analyzed using RT-PCR. (G) BxPC3 or SW1990 cells were infected with lentivirus containing empty or BAG3 construct, and HK2 protein was analyzed using Western blot. A representative image was presented, and the ratio of HK2 expression (normalized by GAPDH; ratio in control cells was defined as 1.0) was noted at the bottom of the image (n = 3). (H and I) Control or BAG3-knockdown BxPC3 (H) or SW1990 (I) cells were plated on E plates and treated with vehicle or 3-BrPA. Real-time cell indexes were analyzed using RTCA. (J and K) BxPC3 (J) or SW1990 (K) cells transduced with lentivirus containing empty or BAG3 construct were plated on E plates and treated with vehicle or 3-BrPA. Real-time cell indexes were analyzed using RTCA.

the potential involvement of IMP3 recruitment in stabilization of HK2 mRNA mediated by BAG3, IMP3 was knocked down using lentivirus containing shRNAs specific against IMP3 (shIMP3). shIMP3 significantly decreased IMP3 mRNA in both control and BAG3-overexpressed BxPC3 cells (Fig. 7 G). IMP3 knockdown significantly decreased HK2 mRNA level in BxPC3 cells with forced BAG3 expression (Fig. 7 H). Unexpectedly, IMP3 knockdown also decreased HK2 mRNA levels in control BxPC3 cells (Fig. 7 H), although it was not recruited to HK2 mRNA (Figs. 6 A and 7 B). As IMP3 is an RBP implicated in regulation of numerous RNA targets, we hypothesized whether BAG3 mRNA might be a target of IMP3. BAG3 mRNA level was then investigated in IMP3-knockdown cells, and we found that IMP3 knockdown decreased BAG3 mRNA in control BxPC3 cells (Fig. 7 I). IMP3 knockdown unaltered BAG3 mRNA in BxPC3 cells with ectopic BAG3 expression (Fig. 7 I). Western blotting confirmed that knockdown of IMP3 decreased HK2 protein levels in both control and BAG3-overexpressing cells (Fig. 7 J). In addition, IMP3 knockdown decreased endogenous BAG3 expression, whereas ectopic BAG3 expression was unaltered (Fig. 7 J). RIP was then performed, and it confirmed that BAG3 transcript was enriched by IMP3 (Fig. 7 K).

Correlation of BAG3 with HK2 expression in pancreatic cancer specimens and BAG3 knock-in (KI) mice

Given that BAG3 might regulate HK2 expression in PDACs, immunohistochemical analyses were performed to evaluate the relationship between BAG3 and HK2 in a pancreatic cancer specimen. BAG3 expression was positively correlated with HK2 expression in pancreatic cancer tissues (Pearson's coefficient test, $r = 0.583$; $P < 0.001$; Fig. 8, A and B). Correlation of BAG3 and HK2 expression was also evaluated in Bag3 KI mice. HK2 was highly expressed in skeletal muscle in control mice, which was further increased in Bag3 KI mice (Fig. 8 C). HK2 expression was small in pancreas, liver, and brain tissues from control mice, whereas it was increased in most tissues from Bag3 KI mice (Fig. 8 C). These data confirm that BAG3 correlated with HK2 expression in vivo. To further confirm regulation of HK2 by BAG3, mouse embryonic fibroblast (MEF) cells were isolated from a control or Bag3 KI embryo. Western blotting demonstrated that BAG3 increased HK2 expression of MEF cells (Fig. 8 D). In addition, BAG3 decreased OCR (Fig. 8 E) and increased ECAR (Fig. 8 F) in MEF cells.

Discussion

Much research has reported a high level of BAG3 expression in cancer cells, and this has been associated with a poor prognosis in patients with PDACs (Rosati et al., 2012). In this study, we used two PDAC cell lines with BAG3 knockdown and overexpression to systemically address the role of BAG3 in aerobic glycolysis in PDAC cells. Down-regulation of BAG3 decreased glycolysis and proliferation of both BxPC3 and SW1990 cells. On the contrary, forced BAG3 overexpression promoted glycolysis and proliferation of PDACs. These data suggest a metabolic mechanism for promotional role of BAG3 on PDAC proliferation.

Among glycolytic enzymes, HK2 particularly favors aerobic glycolysis because of its kinetic features and intracellular distribution (Panasyuk et al., 2012). Although accumulating studies have confirmed that HK2 expression was significantly up-regulated in a variety of malignant tumors including pancreatic cancer (Anderson et al., 2016; Liu et al., 2016; Penny et al., 2016), the molecular mechanisms underlying HK2 up-regulation remain incompletely understood. Our study demonstrates that BAG3 knockdown decreased, whereas BAG3 overexpression increased HK2 expression compared with control cells. Given that HK2 is a critical glycolysis-related enzyme as well as that BAG3 promotes cell proliferation and aerobic glycolysis of PDACs, we sought to determine the mechanisms underlying regulation of HK2 mediated by BAG3. Although the analysis of the transcription of the gene has attracted most of the attention, posttranscriptional mechanisms have increasingly been revealed to be essential steps in the determinant of gene expression levels. It has been reported that PTEN/p53 deficiency selectively enhances expression of HK2 through posttranscriptional and translational regulation (Wang et al., 2014). Our study demonstrates that BAG3 alters HK2 mRNA turnover rather than regulates its transcription.

Every aspect of RNA life, from transcription to transport, storage, and translation, involves protein binding, which results in the formation of RNPs (Müller-McNicoll and Neugebauer, 2013). During gene expression, RBPs recognize many mRNAs and dynamically interact with their cognate mRNAs (Gerstberger et al., 2014). RBPs often participate in multiple posttranscriptional processes and play critical roles in the correct processing and faithful decoding of mRNAs (Gerstberger et al., 2014). To gain specificity, RBPs bind to RNA in collaboration with other RBPs, and a correct interplay between RNAs and RBPs determines the fate of the target mRNA, including RNA trafficking, stability, and translation rate. Three potential RNA-binding domains located at 67–76 aa, 261–294 aa, and 473–485 aa of BAG3 protein were predicted by the Pprint online prediction platform (Kumar et al., 2008). Our study demonstrates that BAG3 was directly recruited to the HK2 transcript via its 67–76 aa and 473–485 aa, assigning a novel function to BAG3 serving as a RBP.

It is well known that the stability and translation of mature mRNAs are controlled by two main types of mRNA-interacting factors: RBPs and miRNAs. Our study found that recruitment of Ago2, the essential effector of miRNA-induced gene silencing, was unaltered, indicating that miRNAs might not be involved in regulation of HK2 mRNA stabilization mediated by BAG3. In silico investigation identified a CDE in the 3′UTR of HK2 mRNA. Our study demonstrates that BAG3 interacts with the CDE of HK2 mRNA and that BAG3 knockdown promoted HK2 mRNA decay via the CDE existing in its 3′UTR. Roquin is a ubiquitously expressed RING-E3 ubiquitin ligase family member and contains a highly conserved ROQ domain required for RNA binding (Glasmacher et al., 2010). It has been reported

(L) Control or BAG3-knockdown BxPC3 cells were transfected with the indicated luciferase reporter vector and a Renilla reporter vector. Luciferase activity was measured 2 d after transfection, and Renilla activity was measured to normalize luciferase activity. (M) BxPC3 cells transduced with lentivirus containing empty or BAG3 construct were transfected with the indicated luciferase reporter vector and a Renilla reporter vector. Luciferase activity was measured 2 d after transfection, and Renilla activity was measured to normalize luciferase activity. *, $P < 0.01$. Error bars indicate means ± SD.

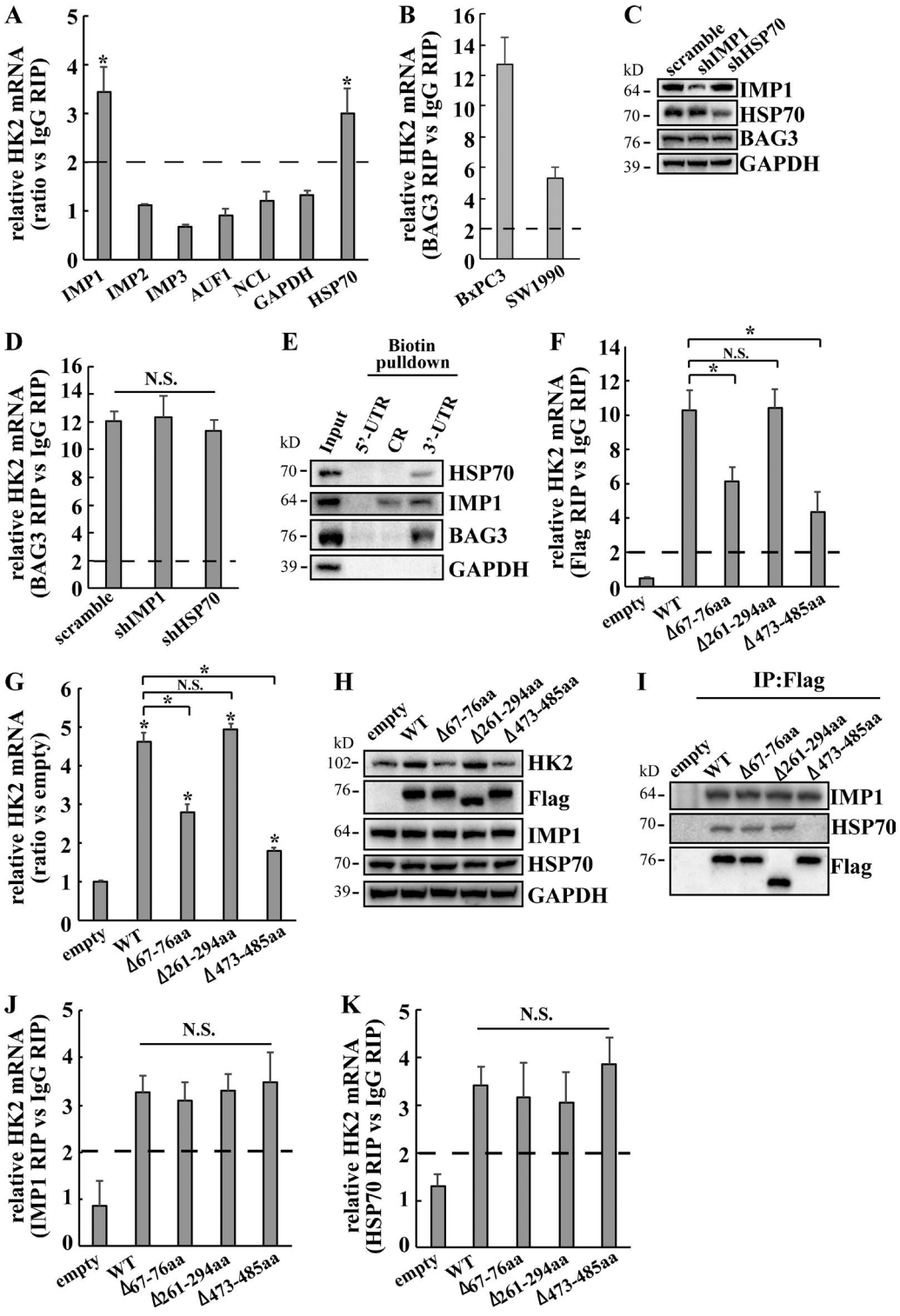

Figure 5. **BAG3 interacts with 3′UTR of HK2 mRNA via its 67–76 aa and 473–486 aa.** (A) RIP was performed using the indicated antibody, and enrichment of HK2 mRNA was measured using RT-qPCR. (B) RIP was performed using lysates from BxPC3 or SW1990 cells with BAG3 antibody, and enrichment of HK2 mRNA was measured using RT-PCR. (C) BxPC3 cells were infected with lentivirus containing shRNAs against IMP1 (shIMP1) or HSP70 (shHSP70), and Western blotting was performed using the indicated antibodies. (D) BxPC3 cells were infected with lentivirus containing shIMP1 or shHSP70, then RIP was performed using BAG3 antibody, and then enrichment of HK2 mRNA was measured using RT-qPCR. (E) Biotinylated RNA segment of HK2 mRNA was used to pull down lysates from BxPC3 cells, and the pulldown materials were analyzed by Western blot analysis using the indicated antibodies. (F–K) BxPC3 cells were infected with lentivirus containing Flag-tagged WT or BAG3 construct with deletion of the potential RNA-binding domain. RIP was performed using Flag antibody to measure HK2 mRNA enrichment (F). HK2 mRNA (G) and protein (H) expression was investigated using RT-qPCR and Western blot, respectively. Interaction of BAG3 and HSP70 or IMP1 was investigated using coimmunoprecipitation (I). Enrichment of HK2 transcript by IMP1 (J) or HSP70 (K) was investigated using RIP. *, $P < 0.01$. Error bars indicate means ± SD. IP, immunoprecipitation.

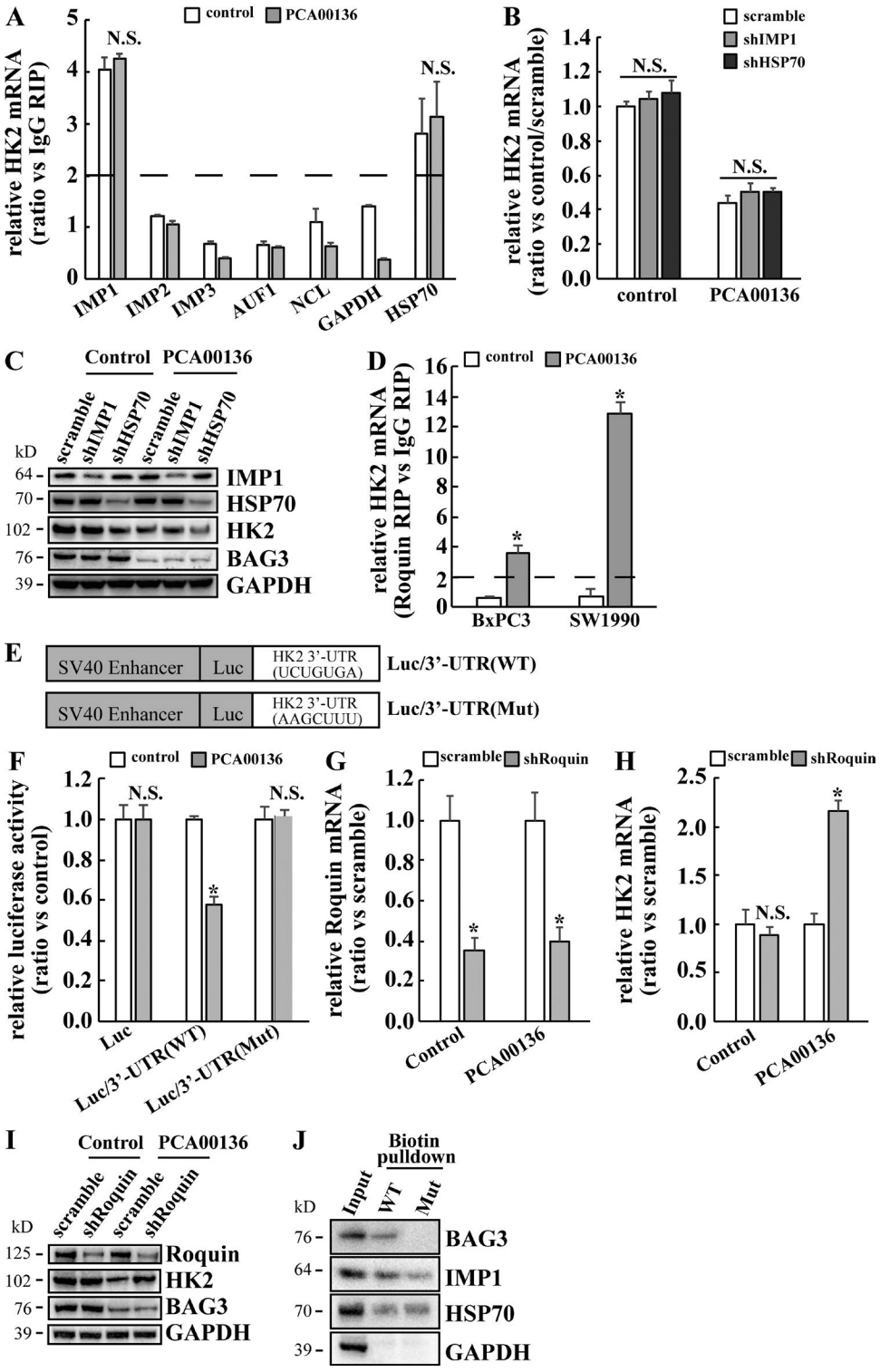

Figure 6. **BAG3 knockdown destabilizes HK2 mRNA via promotion of Roquin recruitment.** (A) RIP was performed using lysates from control or BAG3-knockdown BxPC3 cells with the indicated antibody, and enrichment of HK2 mRNA was measured using RT-PCR. (B and C) Control or BAG3-knockdown BxPC3 cells were infected with shRNAs against IMP1 (shIMP1) or HSP70 (shHSP70) containing lentivirus, and HK2 mRNA (B) and protein (C) was investigated by RT-qPCR and Western blot, respectively. (D) RIP was performed using lysates from BxPC3 or SW1990 cells with Roquin antibody, and enrichment of HK2 mRNA was measured using RT-qPCR. (E) Schematic representation of the luciferase reporter vector bearing WT or CDE mutation (Mut) in the HK2 3′UTR. (F) Control or BAG3-knockdown BxPC3 cells were transfected with the indicated luciferase reporter vector and a Renilla reporter vector. Luciferase activity was measured 2 d after transfection, and Renilla activity was measured to normalize luciferase activity. (G–I) Control or BAG3-knockdown BxPC3 cells were infected with lentivirus containing scramble or shRNA against Roquin (shRoquin). Roquin (G) or HK2 (H) mRNA levels were measured using RT-qPCR. Roquin and HK2 protein levels were analyzed using Western blotting (I). (J) Biotinylated WT or CDE mutation (Mut) HK2 3′UTR mRNA was used to pull down lysates from BxPC3 cells, and the pulldown materials were analyzed by Western blot analysis. *, $P < 0.01$. Error bars indicate means ± SD.

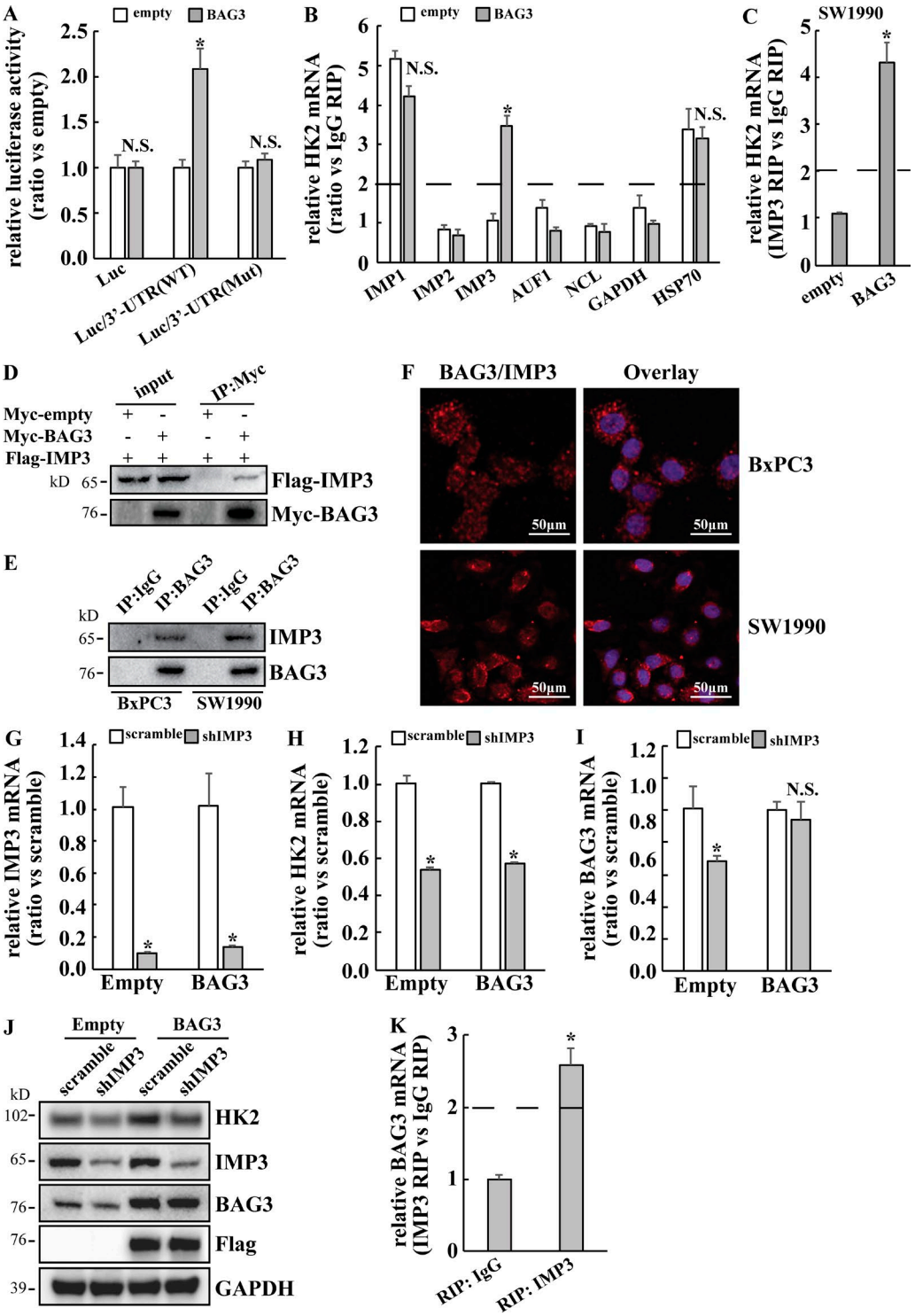

Figure 7. **BAG3 overexpression stabilizes HK2 mRNA via promotion of IMP3 recruitment.** (A) Control or BAG3 overexpression BxPC3 cells were transfected with the indicated luciferase reporter vector and a Renilla reporter vector. Luciferase activity was measured 2 d after transfection, and Renilla activity was measured to normalize luciferase activity. (B) RIP was performed using lysates from BxPC3 cells transduced with empty or BAG3 construct with the indicated antibody, and enrichment of HK2 mRNA was measured using RT-PCR. (C) RIP was performed using lysates from SW1990 cells with IMP3 antibody, and enrichment of HK2 mRNA was measured using RT-PCR. (D) HEK293 cells were cotransfected with BAG3 and IMP3 constructs. Interaction of BAG3 with IMP3 was analyzed using coimmunoprecipitation and subsequent Western blotting. (E) Coimmunoprecipitation was performed using lysates from BxPC3 or SW1990 cells. IP, immunoprecipitation. (F) Direct interaction of endogenous BAG3 with IMP3 was analyzed using DuoLink PLA in BxPC3 or SW1990 cells. (G–J) BxPC3 cells transduced with lentivirus containing empty or BAG3 construct were infected with lentivirus containing scramble or shRNA against IMP3 (shIMP3), and IMP3 (G), HK2 (H), or BAG3 (I) mRNA levels were measured using RT-PCR. Western blots were analyzed using the indicated antibodies (J). (K) RIP was performed using IMP3 antibody with lysates from BxPC3 cells, and enrichment of BAG3 mRNA was measured using RT-PCR. *, $P < 0.01$. Error bars indicate means ± SD.

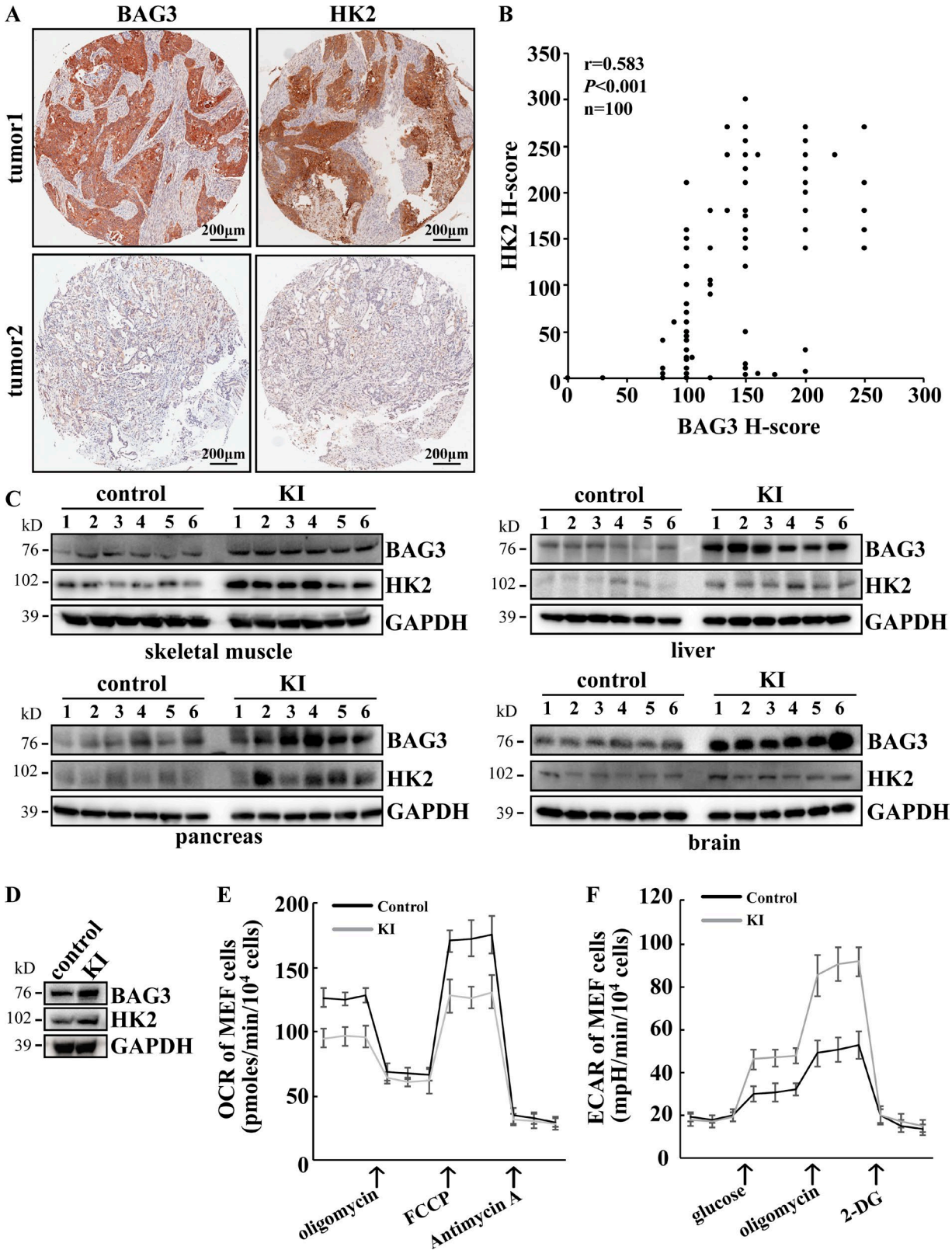

Figure 8. **Correlation of BAG3 and HK2 expression in vivo.** (A) Representative immunohistochemistry staining with BAG3 and HK2 in pancreatic cancer tissues. (B) Scatter plots showing the positive correlation between BAG3 and HK2 IHC scores in pancreatic cancer tissues. Pearson's coefficient tests were performed to assess statistical significance. (C) Western blotting was performed using tissue samples from age-matched mouse littermates without (control) or with transgenic Bag3 KI. (D) MEF cells were isolated from control or Bag3 KI embryos, and HK2 expression was analyzed using Western blotting. (E and F) MEF cells were isolated from control or Bag3 KI embryos, and OCR (E) and ECAR (F) were analyzed using seahorse instrument. Error bars indicate means ± SD. 2-DG, 2-deoxyglucose.

that Roquin recognizes the CDE contained in numerous transcripts and leads to the posttranscriptional miRNA-independent repression of these mRNAs irrespective of the cellular environment (Leppek et al., 2013; Tan et al., 2014; Murakawa et al., 2015). Consistent with these studies, our research demonstrates that BAG3-knockdown miRNA independently suppressed HK2 expression via facilitation of Roquin recruitment to HK2 mRNA.

It is apparent that BAG3 has a wide portfolio of activities that depend strongly on its interaction partners. IGF2 mRBPs (IGF2BPs), also known as IMPs, comprise a family of three mainly cytoplasmic RBPs. IMP1 and IMP3 are oncofetal proteins with high expression observed in various tumors (Bell et al., 2013). Our study demonstrates that ectopic BAG3 overexpression facilitated recruitment of IMP3 to HK2 mRNA via interaction, therefore resulting in stabilization of HK2 mRNA. GST pulldown demonstrated no interaction between recombinant BAG3 and IMP3; however, we did find interaction of endogenous BAG3 and IMP3 in PDACs using DuoLink PLA. Constitutive phosphorylation of BAG3 inside cells may ascribe to the discrepancy observed using recombinant and endogenous proteins.

To the best of our knowledge, this is the first study to describe a novel role of BAG3 in posttranscriptional regulation of HK2 via direct interaction with HK2 mRNA in PDACs. In this study, we show a new mechanism of BAG3 that facilitates proliferation of PDACs by stabilization of HK2 mRNA via competition with Roquin and cooperation with IMP3. Thereby, we give new sights into the complex posttranscriptional regulation of HK2 by BAG3 in PDAC. Notably, we also discover the first cellular mechanism involving BAG3 that functions as a component of the RNA–proteins complex to regulate gene expression at the posttranscriptional level. Our results suggest that targeting BAG3 may result in further treatment avenues in the metabolic modulation of PDAC and merit further investigation in the future.

Materials and methods

Lentiviral vector construction and recombinant lentivirus production

The lentiviral CRISPR/Cas9-mediated BAG3 gene-editing vectors were constructed by annealing gRNA oligonucleotide pairs and subcloning them into a pLenti-Cas9-sgRNA-puro lentivirus vector (GeneChem Co., Ltd.). Genes encoding BAG3 and IMP3 were cloned into a pGC-LV-GV166 lentivirus vector (GeneChem Co., Ltd.). The shRNA targets Ago2, Roquin, IMP1, IMP3, and HSP70 were designed and cloned into a GV118 lentivirus vector (GeneChem Co., Ltd.). DNA sequencing was performed by GeneChem Co., Ltd. to verify the sequence of the insert, and the identities were 100%. After construction, the recombined lentivirus vector, the pHelper 1.0 plasmid, and the pHelper 2.0 plasmid (Invitrogen) were cotransfected into 293T cells using Lipofectamine 2000 (Invitrogen). Recombinant lentiviruses were harvested at 72 h after transfection, centrifuged to get rid of cell debris, and then filtered through a 0.22-µm cellulose acetate filter. Ultimately, a concentrated lentivirus solution was obtained with a final titer of 1.0×10^9 TU/ml.

Knockdown of BAG3 by CRISPR/Cas9

A dual gRNA approach was used to knock down BAG3 by the CRI SPR/Cas9 system. To facilitate the selection of positive clones, a donor vector was generated in such a way that the targeting sequence was replaced by marker genes (GFP and PU, the puromycin resistance gene) once it was integrated into the genomic DNA by homologous recombination. The dual gRNA construct carrying Cas9 and donor vector were introduced into PDAC cells by infection. The empty dual gRNA vector served as a control. 1 wk later, the infected cells were subjected to puromycin selection. Initial identification of knockdown efficiency was performed by genomic PCR followed by RT-PCR and Western blotting.

Cell proliferation assay

Cells were seeded into six-well plates at a density of 100,000 cells per well in 2 ml of medium supplemented with 10% FBS. The medium was changed every day. Cell number at the indicated time points was determined by counting using a hemocytometer.

Growth curve assays using RTCA

Growth curve assays were performed in real time in quadruplicate with the xCELLigence system (ACEA Bioscience) for label-free and real-time monitoring of cell viability as previously described (Li et al., 2014). In brief, 10,000 cells were seeded on RTCA E plates (ACEA Bioscience), and the electrical impedance reflecting a logarithmic relationship to cell number was monitored continuously. Cell growth was reported as the cell index, which is a parameter of cell viability.

OCR and ECAR

20,000 cells were seeded into each well of 24-well assay plates (Seahorse Bioscience) and grown overnight. OCR and ECAR was performed using the Extracellular Flux Analyzer XF24 from Seahorse Bioscience according to the manufacturer's protocol.

Determination of the extracellular lactate

Cells were seeded into 24-well plates. Cells were washed with PBS and then incubated with Krebs-Ringer phosphate Hepes buffer supplemented with 0.2% BSA and 10 mM glucose for 2 h. Then, supernatants were analyzed for their lactate content via an enzyme-coupled fluorescent assay using an L-Lactate Assay kit (Cayman Chemical) according to the manufacturer's instructions. In the assay, lactate dehydrogenase catalyzes the oxidation of lactate to pyruvate along with the concomitant reduction of NAD^+ to NADH. NADH then reacts with the fluorescent substrate to generate a highly fluorescent product, which is analyzed with an excitation wavelength of 530 nm and an emission wavelength of 585 nm. Cell numbers were accounted to normalize extracellular lactate production.

Determination of mRNA half-life

To measure the half-life of endogenous HK2 mRNA, actinomycin D (2 µg/ml) was added into the cell culture medium, and total RNA was prepared at the times indicated and subjected to RT-qPCR analysis using HK2-specific primers. mRNA levels were normalized to 18S rRNA and plotted as a percentage of the value at time 0 (set at 100%).

RIP

The Magna RIP RBP immunoprecipitation kit (EMD Millipore) was used for RIP procedures according to the manufacturer's protocol. In brief, 2×10^7 cells were lysed using RIP lysis buffer, and the supernatant was immunoprecipitated with various antibodies with protein A/G magnetic beads. Magnetic bead–bound complexes were then immobilized with a magnet, and unbound materials were washed off. A/G bead–bound RNA was extracted, and standard RT-qPCR was performed to detect HK2 mRNA in the precipitates.

Generation of reporter vectors and dual luciferase reporter assay

The full-length 5′UTR, CR, or 3′UTR of HK2 was generated by PCR and inserted into the pMIR-REPORT Luciferase vector (Promega) just after

the stop codon. The construct containing mutant for the CDE site was generated using the pMIR-REPORT construct containing a full-length 3′UTR of HK2 by a PCR-based method as recommended in the QuikChange site-directed mutagenesis kit (Agilent Technologies). The transfection was performed with Lipofectamine 2000 according to the manufacturer's instructions. Cells were incubated for 48 h and harvested by adding 100 µl of reporter lysis buffer (Dual-Luciferase Assay system; Promega). The FFL and Renilla luciferase activities were then measured using the Dual-Luciferase Reporter Assay system (Promega) and a luminometer (Mannedorf). FFL activities were normalized by Renilla activities yielding relative activities. All experiments were done in triplicate and were independently performed at least three times to confirm the results. The mean ± SD calculated from one representative experiment was presented.

Label and capture nascent RNA

Newly synthesized RNA was labeled and isolated using Click-iT Nascent RNA Capture kit (Invitrogen) as previously reported (Li et al., 2013). In brief, cells were incubated with 0.2 mM of 5-ethymyl uridine for 4 h to label nascent RNA. Total RNA was isolated using TRIzol reagent, and the 5-ethymyl uridine–labeled nascent RNA was biotinylated in Click-iT reaction buffer with 0.5 mM of biotin azide. The biotinylated nascent RNA was subsequently captured on streptavidin magnetic beads.

Western blot analysis

Total cellular proteins were extracted using lysis buffer containing 20 mM Tris-HCl, 150 mM NaCl, 2 mM EDTA, 1% Triton X-100, and protease inhibitor cocktail (Sigma-Aldrich). Extracted proteins were quantified using the BCA protein assay kit. 20 µg of total protein was separated using 12% SDS-PAGE and transferred to polyvinylidene difluoride membrane (EMD Millipore). The following antibodies were used in this study: Roquin-1, IMP2, IMP3, AUF1, NCL, HK2, and GAP DH (EMD Millipore); IMP1 and BAG6 (Cell Signaling Technology); BAG1 (Novus Biologicals); BAG2 (Abcam); and BAG3 (GeneTex).

Biotin pulldown assay

Luciferase vector containing WT or mutant 3′UTR of HK2 mRNA was used as a template for the PCR amplification. All 5′ primers contained the T7 promoter sequence 5′-CCAAGCTTCTAATACGACTCACTA TAGGGAG-3′ (T7). For biotin pulldown assays, PCR-amplified DNA was used as the template to transcribe biotinylated RNA by using T7 RNA polymerase in the presence of biotin-UTP. RNA–protein binding reactions were performed using 500 µg cell lysates and 1 µg biotin-labeled RNA in a final volume of 20 µl using binding buffer A (20 mM Hepes-KOH, pH 7.5, 2.5 mM $MgCl_2$, 100 mM KCl, 20% glycerol, 0.5 mM dithiothreitol, and protease inhibitor tablets). Reaction mixtures were incubated for 1 h at room temperature. Complexes were isolated with paramagnetic streptavidin-conjugated DynaBeads (Invitrogen), and the pulldown materials were analyzed by Western blotting analysis.

Tissue microarray and immunohistochemical staining

Tissue microarray sections were purchased from Shanghai Outdo Biotech Co., Ltd. Tissue sections were immunostained with antibodies to BAG3 and HK2. A semiquantitative H score range was calculated for each specimen by multiplying the distribution areas (0–100%) at each staining intensity level by the intensities (0, negative; 1, weak staining; 2, moderate staining; and 3, strong staining) as previously reported (Detre et al., 1995). The median value of the H score was chosen as the cutoff criterion to dichotomize into high- and low-expression subgroups.

Generation of Rosa26-Bag3 KI mice

Rosa26-Bag3 KI mice were generated on C57BL/6 background by Shanghai Biomodel Organism Science and Technology Development Co., Ltd. Rosa26-Bag3 KI mice were then crossbred with EIIa-Cre C57BL/6 mice to obtain mice with widely expressed Bag3. In three successive breeding steps, cohorts of littermates with or without transgenic Bag3 expression were generated in ratios consistent with Mendelian principles. 24–26-wk-old littermate mice (female, weight 24–32 g) were used in all experiments. All procedures involving animals conformed to the guidelines of the Institutional Animal Care Committee of China Medical University.

Nude mice xenograft experiments

BALB/c-nu/nu mice (4–5 wk old, female) were purchased from Shanghai Laboratory Animal Center (Chinese Academy of Science). All animal procedures were approved and compiled with the guidelines of the Institutional Animal Care Committee of China Medical University. BxPC3 cells were infected with lentivirus containing control or PCA00136 gRNA. Mice were subcutaneously inoculated with 10^7 viable cells. 10 mice per cell line were used. On day 28, the mice were sacrificed by overdose of sodium pentobarbital, and primary tumors were excised and weighed.

Isolation and culture of MEF cells

Pregnant mice at 13 or 14 d after coitum were sacrificed by cervical dislocation, and each embryo was separated from its placenta and embryonic sac. Head and red organs were dissected for genotyping, and the remained tissues were minced and incubated with 0.05% trypsin/EDTA containing DNase I. Isolated cells were transferred to a T150 (TPP) flask coated with 0.2% gelatin (gelatin from bovine skin; Type B; Sigma-Aldrich) for 2 h. The fibroblast cells (passage 0; P0) are the only cells that have ability to attach to the gelatin-coated flasks. Primary MEF cells with three to five passages were used for the experiments.

Statistics

The statistical significance of the difference was analyzed by ANO VA and Dunnett's post hoc test. Statistical significance was defined as $P < 0.05$. All experiments were repeated three times, and data were expressed as means ± SD from a representative experiment.

Online supplemental material

Fig. S1 displays how BAG3 knockdown mediated by another gRNA PCA00137 increases OCR, whereas it decreases ECAR in PDACs. Fig. S2 demonstrates how the HK inhibitor 3-BrPA decreases OCR and ECAR in PDACs. Fig. S3 shows how regulation of HK2 mRNA by BAG3 is in an miRNA–independent manner.

Acknowledgments

This work was partly supported by National Natural Science Foundation of China (81572828 and 81602439) and distinguished professor of LNET 2014.

The authors declare no competing financial interests.

Author contributions: M.-X. An, H.-B. Yao, and C. Li performed all molecular biology and imaging experiments. S. Li and X.-N. Meng performed animal experiments. J. Sun established the CRISPR/Cas9 BAG3-knockdown cells. J.-M. Wang and X.-Y. Li performed MEF isolation and identification. H.-Q. Wang and M.-X. An designed the experiments and wrote the manuscript.

Submitted: 10 January 2017
Revised: 15 May 2017
Accepted: 18 September 2017

References

Anderson, M., R. Marayati, R. Moffitt, and J.J. Yeh. 2016. Hexokinase 2 promotes tumor growth and metastasis by regulating lactate production in pancreatic cancer. *Oncotarget.* 8:56081–56094.

Behl, C. 2016. Breaking BAG: The Co-Chaperone BAG3 in Health and Disease. *Trends Pharmacol. Sci.* 37:672–688. https://doi.org/10.1016/j.tips.2016.04.007

Bell, J.L., K. Wächter, B. Mühleck, N. Pazaitis, M. Köhn, M. Lederer, and S. Hüttelmaier. 2013. Insulin-like growth factor 2 mRNA-binding proteins (IGF2BPs): post-transcriptional drivers of cancer progression? *Cell. Mol. Life Sci.* 70:2657–2675. https://doi.org/10.1007/s00018-012-1186-z

Cairns, R.A., I.S. Harris, and T.W. Mak. 2011. Regulation of cancer cell metabolism. *Nat. Rev. Cancer.* 11:85–95. https://doi.org/10.1038/nrc2981

Chiappetta, G., M. Ammirante, A. Basile, A. Rosati, M. Festa, M. Monaco, E. Vuttariello, R. Pasquinelli, C. Arra, M. Zerilli, et al. 2007. The antiapoptotic protein BAG3 is expressed in thyroid carcinomas and modulates apoptosis mediated by tumor necrosis factor-related apoptosis-inducing ligand. *J. Clin. Endocrinol. Metab.* 92:1159–1163. https://doi.org/10.1210/jc.2006-1712

DeBerardinis, R.J., and C.B. Thompson. 2012. Cellular metabolism and disease: what do metabolic outliers teach us? *Cell.* 148:1132–1144. https://doi.org/10.1016/j.cell.2012.02.032

Detre, S., G. Saclani Jotti, and M. Dowsett. 1995. A "quickscore" method for immunohistochemical semiquantitation: validation for oestrogen receptor in breast carcinomas. *J. Clin. Pathol.* 48:876–878. https://doi.org/10.1136/jcp.48.9.876

Fabian, M.R., N. Sonenberg, and W. Filipowicz. 2010. Regulation of mRNA translation and stability by microRNAs. *Annu. Rev. Biochem.* 79:351–379. https://doi.org/10.1146/annurev-biochem-060308-103103

Felzen, V., C. Hiebel, I. Koziollek-Drechsler, S. Reißig, U. Wolfrum, D. Kögel, C. Brandts, C. Behl, and T. Morawe. 2015. Estrogen receptor α regulates non-canonical autophagy that provides stress resistance to neuroblastoma and breast cancer cells and involves BAG3 function. *Cell Death Dis.* 6:e1812. https://doi.org/10.1038/cddis.2015.181

Festa, M., L. Del Valle, K. Khalili, R. Franco, G. Scognamiglio, V. Graziano, V. De Laurenzi, M.C. Turco, and A. Rosati. 2011. BAG3 protein is overexpressed in human glioblastoma and is a potential target for therapy. *Am. J. Pathol.* 178:2504–2512. https://doi.org/10.1016/j.ajpath.2011.02.002

Gamerdinger, M., P. Hajieva, A.M. Kaya, U. Wolfrum, F.U. Hartl, and C. Behl. 2009. Protein quality control during aging involves recruitment of the macroautophagy pathway by BAG3. *EMBO J.* 28:889–901. https://doi.org/10.1038/emboj.2009.29

Gatenby, R.A., and R.J. Gillies. 2004. Why do cancers have high aerobic glycolysis? *Nat. Rev. Cancer.* 4:891–899. https://doi.org/10.1038/nrc1478

Gerstberger, S., M. Hafner, and T. Tuschl. 2014. A census of human RNA-binding proteins. *Nat. Rev. Genet.* 15:829–845. https://doi.org/10.1038/nrg3813

Glasmacher, E., K.P. Hoefig, K.U. Vogel, N. Rath, L. Du, C. Wolf, E. Kremmer, X. Wang, and V. Heissmeyer. 2010. Roquin binds inducible costimulator mRNA and effectors of mRNA decay to induce microRNA-independent post-transcriptional repression. *Nat. Immunol.* 11:725–733. https://doi.org/10.1038/ni.1902

Hanahan, D., and R.A. Weinberg. 2011. Hallmarks of cancer: the next generation. *Cell.* 144:646–674. https://doi.org/10.1016/j.cell.2011.02.013

Kong, D.H., Q. Zhang, X. Meng, Z.H. Zong, C. Li, B.Q. Liu, Y. Guan, and H.Q. Wang. 2013. BAG3 sensitizes cancer cells exposed to DNA damaging agents via direct interaction with GRP78. *Biochim. Biophys. Acta.* 1833:3245–3253. https://doi.org/10.1016/j.bbamcr.2013.09.013

Kong, D.H., S. Li, Z.X. Du, C. Liu, B.Q. Liu, C. Li, Z.H. Zong, and H.Q. Wang. 2016. BAG3 elevation inhibits cell proliferation via direct interaction with G6PD in hepatocellular carcinomas. *Oncotarget.* 7:700–711. https://doi.org/10.18632/oncotarget.6396

Kumar, M., M.M. Gromiha, and G.P.S. Raghava. 2008. Prediction of RNA binding sites in a protein using SVM and PSSM profile. *Proteins.* 71:189–194.

Leppek, K., J. Schott, S. Reitter, F. Poetz, M.C. Hammond, and G. Stoecklin. 2013. Roquin promotes constitutive mRNA decay via a conserved class of stem-loop recognition motifs. *Cell.* 153:869–881. https://doi.org/10.1016/j.cell.2013.04.016

Li, C., S. Li, D.H. Kong, X. Meng, Z.H. Zong, B.Q. Liu, Y. Guan, Z.X. Du, and H.Q. Wang. 2013. BAG3 is upregulated by c-Jun and stabilizes JunD. *Biochim. Biophys. Acta.* 1833:3346–3354. https://doi.org/10.1016/j.bbamcr.2013.10.007

Li, S., H.Y. Zhang, T. Wang, X. Meng, Z.H. Zong, D.H. Kong, H.Q. Wang, and Z.X. Du. 2014. BAG3 promoted starvation-induced apoptosis of thyroid cancer cells via attenuation of autophagy. *J. Clin. Endocrinol. Metab.* 99:E2298–E2307. https://doi.org/10.1210/jc.2014-1779

Liao, Q., F. Ozawa, H. Friess, A. Zimmermann, S. Takayama, J.C. Reed, J. Kleeff, and M.W. Büchler. 2001. The anti-apoptotic protein BAG-3 is overexpressed in pancreatic cancer and induced by heat stress in pancreatic cancer cell lines. *FEBS Lett.* 503:151–157. https://doi.org/10.1016/S0014-5793(01)02728-4

Liu, Y., K. Wu, L. Shi, F. Xiang, K. Tao, and G. Wang. 2016. Prognostic Significance of the Metabolic Marker Hexokinase-2 in Various Solid Tumors: A Meta-Analysis. *PLoS One.* 11:e0166230. https://doi.org/10.1371/journal.pone.0166230

Meng, X., D.H. Kong, N. Li, Z.H. Zong, B.Q. Liu, Z.X. Du, Y. Guan, L. Cao, and H.Q. Wang. 2014. Knockdown of BAG3 induces epithelial-mesenchymal transition in thyroid cancer cells through ZEB1 activation. *Cell Death Dis.* 5:e1092. https://doi.org/10.1038/cddis.2014.32

Müller-McNicoll, M., and K.M. Neugebauer. 2013. How cells get the message: dynamic assembly and function of mRNA-protein complexes. *Nat. Rev. Genet.* 14:275–287. https://doi.org/10.1038/nrg3434

Murakawa, Y., M. Hinz, J. Mothes, A. Schuetz, M. Uhl, E. Wyler, T. Yasuda, G. Mastrobuoni, C.C. Friedel, L. Dölken, et al. 2015. RC3H1 post-transcriptionally regulates A20 mRNA and modulates the activity of the IKK/NF-κB pathway. *Nat. Commun.* 6:7367. https://doi.org/10.1038/ncomms8367

Panasyuk, G., C. Espeillac, C. Chauvin, L.A. Pradelli, Y. Horie, A. Suzuki, J.S. Annicotte, L. Fajas, M. Foretz, F. Verdeguer, et al. 2012. PPARγ contributes to PKM2 and HK2 expression in fatty liver. *Nat. Commun.* 3:672. https://doi.org/10.1038/ncomms1667

Penny, H.L., J.L. Sieow, G. Adriani, W.H. Yeap, P. See Chi Ee, B. San Luis, B. Lee, T. Lee, S.Y. Mak, Y.S. Ho, et al. 2016. Warburg metabolism in tumor-conditioned macrophages promotes metastasis in human pancreatic ductal adenocarcinoma. *OncoImmunology.* 5:e1191731. https://doi.org/10.1080/2162402X.2016.1191731

Romano, M.F., M. Festa, G. Pagliuca, R. Lerose, R. Bisogni, F. Chiurazzi, G. Storti, S. Volpe, S. Venuta, M.C. Turco, and A. Leone. 2003a. BAG3 protein controls B-chronic lymphocytic leukaemia cell apoptosis. *Cell Death Differ.* 10:383–385. https://doi.org/10.1038/sj.cdd.4401167

Romano, M.F., M. Festa, A. Petrella, A. Rosati, M. Pascale, R. Bisogni, V. Poggi, E.C. Kohn, S. Venuta, M.C. Turco, and A. Leone. 2003b. BAG3 protein regulates cell survival in childhood acute lymphoblastic leukemia cells. *Cancer Biol. Ther.* 2:508–510. https://doi.org/10.4161/cbt.2.5.524

Rosati, A., M. Ammirante, A. Gentilella, A. Basile, M. Festa, M. Pascale, L. Marzullo, M.A. Belisario, A. Tosco, S. Franceschelli, et al. 2007. Apoptosis inhibition in cancer cells: a novel molecular pathway that involves BAG3 protein. *Int. J. Biochem. Cell Biol.* 39:1337–1342. https://doi.org/10.1016/j.biocel.2007.03.007

Rosati, A., V. Graziano, V. De Laurenzi, M. Pascale, and M.C. Turco. 2011. BAG3: a multifaceted protein that regulates major cell pathways. *Cell Death Dis.* 2:e141. https://doi.org/10.1038/cddis.2011.24

Rosati, A., S. Bersani, F. Tavano, E. Dalla Pozza, M. De Marco, M. Palmieri, V. De Laurenzi, R. Franco, G. Scognamiglio, R. Palaia, et al. 2012. Expression of the antiapoptotic protein BAG3 is a feature of pancreatic adenocarcinoma and its overexpression is associated with poorer survival. *Am. J. Pathol.* 181:1524–1529. https://doi.org/10.1016/j.ajpath.2012.07.016

Sherman, M.Y., and V.L. Gabai. 2015. Hsp70 in cancer: back to the future. *Oncogene.* 34:4153–4161. https://doi.org/10.1038/onc.2014.349

Suzuki, M., M. Iwasaki, A. Sugio, A. Hishiya, R. Tanaka, T. Endo, S. Takayama, and T. Saito. 2011. BAG3 (BCL2-associated athanogene 3) interacts with MMP-2 to positively regulate invasion by ovarian carcinoma cells. *Cancer Lett.* 303:65–71. https://doi.org/10.1016/j.canlet.2011.01.019

Takayama, S., Z. Xie, and J.C. Reed. 1999. An evolutionarily conserved family of Hsp70/Hsc70 molecular chaperone regulators. *J. Biol. Chem.* 274:781–786. https://doi.org/10.1074/jbc.274.2.781

Tan, D., M. Zhou, M. Kiledjian, and L. Tong. 2014. The ROQ domain of Roquin recognizes mRNA constitutive-decay element and double-stranded RNA. *Nat. Struct. Mol. Biol.* 21:679–685. https://doi.org/10.1038/nsmb.2857

Vander Heiden, M.G., L.C. Cantley, and C.B. Thompson. 2009. Understanding the Warburg effect: the metabolic requirements of cell proliferation. *Science.* 324:1029–1033. https://doi.org/10.1126/science.1160809

Wang, L., H. Xiong, F. Wu, Y. Zhang, J. Wang, L. Zhao, X. Guo, L.J. Chang, Y. Zhang, M.J. You, et al. 2014. Hexokinase 2-mediated Warburg effect is required for PTEN- and p53-deficiency-driven prostate cancer growth. *Cell Reports.* 8:1461–1474. https://doi.org/10.1016/j.celrep.2014.07.053